Angle-resolved Auger-photoelectron coincidence spectroscopy (AR-APECS) of the Ge(100) surface

R. Gotter,[1] A. Ruocco,[2] M. T. Butterfield,[3] S. Iacobucci,[4] G. Stefani,[2] and R. A. Bartynski[3]
[1]*Laboratorio Nazionale TASC-INFM, Area Science Park, SS 14 km 163.5, Basovizza I-34012 Trieste, Italy*
[2]*Dipartimento di Fisica and UnitàINFM Università di Roma Tre, Via della Vasca Navale 84, I-00146 Roma, Italy*
[3]*Department of Physics and Astronomy and Laboratory for Surface Modification, Rutgers University, 136 Frelinghuysen Road, Piscataway, New Jersey 08855*
[4]*Istituto Metodologie Avanzate Inorganiche CNR and Unità INFM Roma 3, Area della ricerca di Roma, CP 16, I-00016 Monterotondo, Italy*
(Received 18 October 2002; published 21 January 2003)

We have measured the angular distribution of Ge $L_3M_{45}M_{45}$ Auger electrons in coincidence with Ge $2p_{3/2}$ core photoelectrons along the (001) azimuth of the Ge(100) surface. Intensity modulations arising from diffraction effects are suppressed in the coincidence Auger angular distribution and, when specific emission angles of the photoelectrons are considered, new features appear. We attribute the former effect to enhanced surface specificity of the coincidence technique and the latter to sensitivity of the coincidence measurement to alignment of the core hole state.

DOI: 10.1103/PhysRevB.67.033303 PACS number(s): 68.49.−h, 78.70.−g, 79.60.−i

Auger electron spectroscopy (AES) and core-level photoelectron spectroscopy (XPS) are two of the most widely used techniques for the characterization of materials and their surfaces. The electron emission phenomena upon which these spectroscopies are based are closely related in that the core hole left behind by the photoelectron is filled during the Auger decay process. Only recently with the development of Auger-photoelectron coincidence spectroscopy (APECS) has this connection been exploited. In APECS the core photoelectron is measured in time coincidence with its associated Auger electron. This ensures that both electrons are generated in the same photoexcitation event. APECS has been used to probe electron emission from solids with unprecedented discrimination in measurements that (i) isolate individual sites in a solid and probe their local atomic structure,[1,2] (ii) separate overlapping multiplet structures,[3] (iii) eliminate uncorrelated secondary electron background,[4] (iv) eliminate core-level lifetime broadening of spectral features,[5] and (v) distinguish between ''intrinsic'' and ''extrinsic'' secondary electron emission. All of these results have been achieved by measuring, in time coincidence, the energy distribution of photoexcited Auger electron-photoelectron pairs that are simultaneously emitted from a solid.

The amount of information obtained from photoemission spectra is vastly increased when one measures the angular distribution of photoemitted electrons as well as their energy. For example, ultraviolet photoemission spectroscopy (UPS) gives information about the valence-band density of states of a solid, while *angle-resolved* UPS enables one to directly map the energy bands. Similarly, from XPS and AES one can obtain information about the chemical state of a surface, while *angle-resolved* measurements [i.e., x-ray photoelectron diffraction (XPD) and Auger electron diffraction (AED)] enable one to perform surface structural measurements and produce holographic images of surface geometry. In a similar way, *angle-resolved* APECS (i.e., AR-APECS) is expected to add an important level of discrimination to the APECS technique. This has been demonstrated for free atoms by an AR-APECS investigation of resonant double photoionization in gas phase Ne,[6] which exhibited combined effects of post-collisional interaction and interference due to indistinguishability of the electrons in the final state. Recently, we have initiated AR-APECS studies of the angular distribution of correlated electron pairs emitted from solid surfaces.[7] Our efforts have been aimed at determining if atomic effects survive the solid-state environment, and establishing what phenomena might be observed in such measurements in the condensed phase.

In this paper we describe the results of an of AR-APECS experiment where the Ge $L_3M_{45}M_{45}$ Auger electron angular distribution was measured in coincidence with Ge $2p_{3/2}$ core photoelectrons from the Ge(100) surface. These are the first AR-APECS measurements from a solid surface that definitively demonstrate that the angular distribution of Auger electrons measured in coincidence with core photoelectrons differs from the noncoincidence, or singles, angular distribution. We find that differences between the coincidence and noncoincidence distributions arise from the increased surface specificity of the coincidence technique. The observation of features in the Auger distribution suggests that the coincidence core photoelectron specifies the electronic alignment of the ion, which in turn is reflected in the angular distribution of Auger electrons.

The measurements were performed using the unique capabilities of the ALOISA beamline at the ELETTRA synchrotron in Trieste, Italy. The experimental setup is discussed in detail elsewhere[8] and only a brief description will be given here. A monochromatized beam ($h\nu = 1450$ eV) of linearly polarized photons is impinged at a grazing angle of 6° and nearly *p* polarized onto a Ge(100) single-crystal surface that had been sputtered and annealed until it exhibited a sharp reflection high-energy electron-diffraction pattern indicating the well-known (2×1) reconstruction.[9] The measurement chamber contains an array of seven electron analyzers, arranged in two independent rotatable frames (two analyzers on the so-called bimodal frame and five on the axial frame) that were used to detect electrons at preset energies and

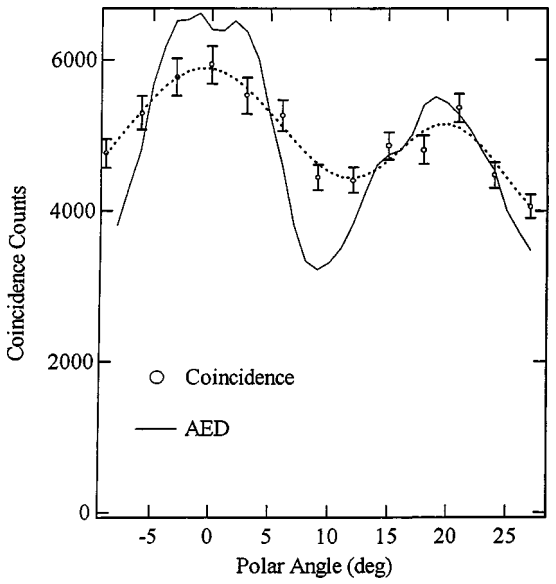

FIG. 1. Integrated angular distribution of Ge $L_3M_{45}M_{45}$ Auger electrons along the (001) azimuth of the Ge(100) surface, measured in coincidence with Ge $2p_{3/2}$ core photoelectrons and a simultaneously acquired AED pattern. The heavy curve is a guide to the eye through the coincidence data.

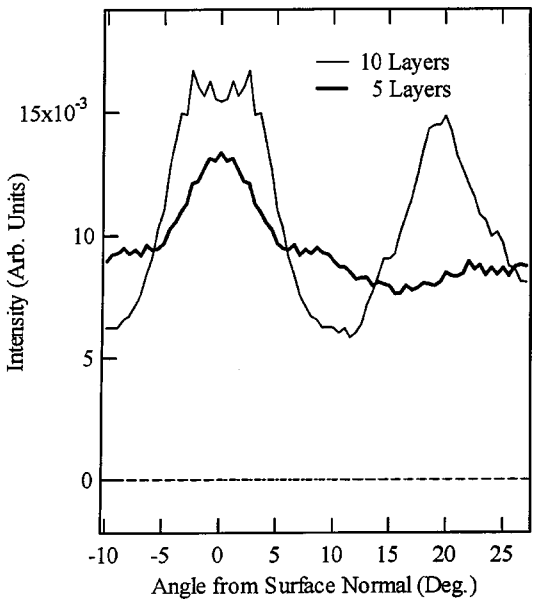

FIG. 2. Calculated angular distribution of Ge $L_3M_{45}M_{45}$ Auger electrons along the (001) azimuth of the Ge(100) surface with emitters in the first ten and the first five layers of the surface.

angles. The two analyzers on the bimodal (or scanning) frame were rotated as a unit to monitor the Ge $L_3M_{45}M_{45}(^1G)$ Auger electron emission intensity (at a kinetic energy of 1362 eV) as a function of polar angle. The other five analyzers, placed at intervals of 18° on the axial (or fixed) frame, were tuned to monitor Ge $2p_{3/2}$ photoelectrons (at a kinetic energy of 252 eV) in a plane that contained the photon beam axis and that was rotated 54° from the sample normal. In this way the two bimodal analyzers measured an angular distribution in coincidence with five different values of the photoelectron momentum wave vector selected by the five axial analyzers. With an energy resolution of 2 eV, the spin-orbit splitting of the core level in photoemission, as well as the dominant ^1G multiplet of the Auger transition, were resolved easily. The experimental data were acquired in two modes: an *integrated* mode where an Auger electron was detected by one of the bimodal analyzers and a photoelectron was detected in *any* of the five axial analyzers, and a *pairwise* mode where an Auger electron detected in one of the bimodal analyzers comes in coincidence with photoelectrons in only one particular axial analyzer. In both modes, timing spectra for each pair of analyzers, covering a range of several hundred nanoseconds an either side of $\Delta t = 0$, were recorded so that the accidental contribution to the coincidence signal could be determined and subtracted to produce the true coincidence signal, which is reported here. We simultaneously recorded a noncoincidence, or singles, AED pattern during the AR-APECS measurement.

The intensity of the Ge $L_3M_{45}M_{45}$ (^1G) Auger line as a function of polar angle along the (001) azimuth of the Ge(100) surface is presented in Fig. 1. The solid curve is the singles angular distribution, which is characterized by a strong peak near normal emission ($\theta = 0°$), a local minimum near $\theta = 10°$, followed by a second local maximum near $\theta = 20°$. The singles Auger angular distribution can be understood in terms of AED. In Fig. 2 we plot the results of a multiple scattering[10] calculation for the (2×1) reconstructed Ge(100) surface. The thin curve is the result of the calculation performed with emitter atoms in the first ten layers of a Ge(100) cluster. The coordinates of atoms in the first two layers were taken from a recent x-ray-diffraction measurement of this surface[11] while atoms in other layers assumed their bulk positions. The calculation does a good job of reproducing the two prominent features, at $\theta = 0°$ and $\theta = 20°$, that correspond to forward focusing along the $\langle 001 \rangle$ and $\langle 013 \rangle$ crystallographic directions, respectively.

The angular distribution of Ge $L_3M_{45}M_{45}$ Auger electrons measured in coincidence with Ge $2p_{3/2}$ core-level photoelectrons acquired in the integrated mode is shown as the data points with error bars in Fig. 1. The dashed curve is a guide to the eye. It is clear that the coincidence polar scan differs substantially from the singles distribution: maxima and minima are roughly at the same angles but the amplitude of the modulation is significantly smaller than that of the noncoincidence distribution.

Since AED is primarily responsible for the shape of the singles distribution, we investigate how performing a coincidence measurement might modify this effect. It is well known that, owing to the fact that both the Auger electron and the photoelectron must escape the solid for a coincidence event to be detected, APECS is about twice as surface sensitive as singles spectroscopy.[4,12] We simulate this effect by repeating our calculation with the same geometry, but including emitters in only the first five atomic layers. The result, given as the heavy curve of Fig. 2, exhibits the same suppression of modulation exhibited by the coincidence distribution reported in Fig. 1, giving evidence that the enhanced surface sensitivity of APECS is responsible for this observation. From the point of view of surface structure, these re-

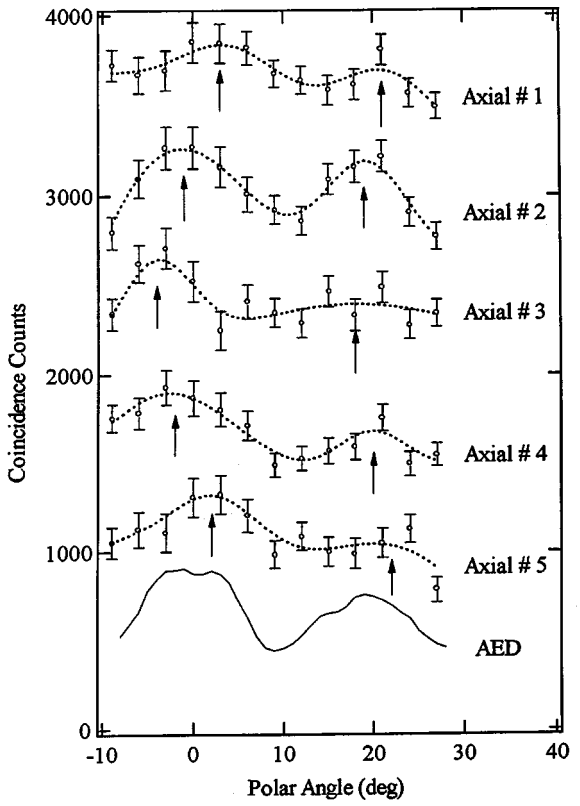

FIG. 3. Pairwise AR-APECS angular distributions of Ge $L_3M_{45}M_{45}$ Auger electrons measured in coincidence with Ge $2p_{3/2}$ core photoelectrons detected in each of the five axial electron energy analyzers. The AED and the coincidence data associated with axial analyzer number 5 are referenced to zero, while the other curves are shifted upward for clarity of presentation.

sults show that AR-APECS could have direct applications to thin-film multilayer systems where signals from the substrate would obscure emission from the overlayer in singles AED.

More interesting observations, the implications of which go beyond surface sensitivity, are made when we consider the coincidence angular distributions obtained in the pairwise mode. In Fig. 3, we display the Auger angular distribution as obtained in coincidence with five different directions of the photoelectron momentum. The data points with error bars are the coincidence distribution and the dashed line is a guide to the eye. The thin solid curve is the simultaneously acquired AED pattern. Although these coincidence data have larger error bars than the integrated data, the differences with respect to the AED pattern are now even more pronounced. Systematic changes are observed between the profiles obtained for neighboring analyzer pairs. Regarding the maximum near $\theta=0°$, the curves from analyzers 1 and 5 show maxima that are clearly on the positive-angle side of the surface normal while the peak for analyzer 3 is on the negative side. The curves for analyzers 2 and 4 are intermediate in this respect. Although less pronounced, the feature near $\theta=20°$ appears to exhibit a similar trend. These findings cannot be ascribed to enhanced surface sensitivity since if that were the case, all pairs would display identical angular distributions.

The differences between these pairwise coincidence distributions can be understood using a stepwise model for the photoemission process whereby core hole generation, Auger emission, and diffraction are treated independently. This approach is justified by the long lifetime of the core hole and the well-defined parity and angular momentum of the final state.[13] Within this framework, the XPD (AED) pattern is generated when the atomic wave function of the ejected electron, the so-called ''source function,'' is diffracted by the crystal lattice.[14,15] The photoelectron and Auger electron source functions are characterized by the angular momentum and magnetic quantum numbers l_p, m_p and l_A, m_A, respectively, and give an initial angular distribution in terms of the wave-function symmetry of the emitted electrons. Subsequent scattering from the lattice determines the detailed modulation of the angular pair intensity distribution in terms of the arrangement of neighboring atoms. The full XPD (AED) pattern is then obtained by summing the contribution of the individual diffracted partial waves over quantum numbers l_p (l_A) and m_p (m_A). Naturally, the Auger pattern is linked to the photoelectron pattern by dipole and Coulomb matrix elements. Linear photon polarization ensures $m_c=m_p$, where the subscript c refers to the core hole. Furthermore, the following selection rules[16] for Auger decay relate the quantum numbers of the Auger electron to those of the core hole:

$$l_c-|l_1-l_2|\leqslant l_A\leqslant l_c+l_1+l_2, \tag{1}$$

$$l_c+l_1+l_2+l_A=\text{even}, \tag{2}$$

$$m_c+m_1=m_2+m_A. \tag{3}$$

Here subscripts 1 and 2 refer to the two holes of the final state. In our experiment, we are detecting a $2p$ photoelectron, so $l_c=1$. Furthermore, the $L_3M_{45}M_{45}$ Auger transition leaves two $3d$ holes (i.e., $l_1=l_2=2$) in the final state. From this we find that Eq. (1) implies that $1\leqslant l_A\leqslant 5$ and Eq. (2) implies that l_A is odd. Therefore, l_A may assume the value of 1, 3, or 5. AED studies of similar transitions indicate that the Auger electron is predominantly $l_A=3$. Consequently we can limit the values of its magnetic quantum number to $m_A=0$, ±1, ±2, and ±3, while $l_c=1$ means the possible values of m_c are 0 and ±1. This combined with Eq. (3) enables us to specify that

$$m_A=(m_1-m_2) \quad \text{if } m_c=0, \tag{4}$$

$$m_A=(m_1-m_2)+1 \quad \text{if } m_c=+1, \tag{5}$$

$$m_A=(m_1-m_2)-1 \quad \text{if } m_c=-1. \tag{6}$$

In the coincidence measurement, we detect only Auger electrons associated with the $^1G_4$ configuration of the two-hole final state. Therefore, the Auger final state has $L=4$ and $m_L=0$, ±1, ±2, ±3, and ±4. These sublevels are given by the particular combinations of $|l_1,m_1\rangle|l_2,m_2\rangle$ product states specified by the appropriate Clebsch-Gordan coefficients. We can therefore determine the relative probability for each possible value of m_A for a given value of m_c. These probabilities are summarized in Fig. 4. In our coincidence measure-

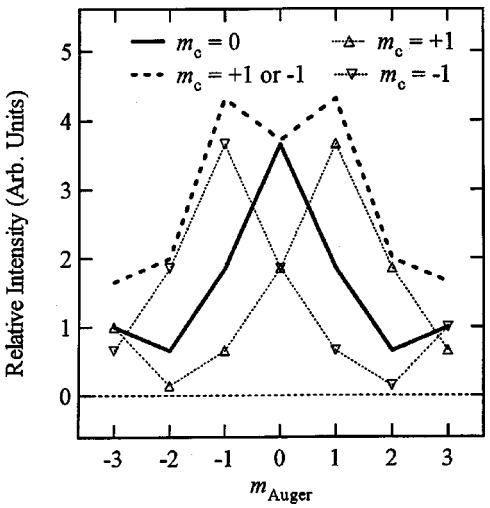

FIG. 4. Relative probability of different magnetic quantum numbers for the Auger electron m_A, for a given value of the magnetic quantum number of the core hole m_c, and for the $^1G_4$ term of the Ge $L_3M_{45}M_{45}$ Auger transition.

ments, the five axial analyzers detected photoelectrons at different emission angles, and therefore will have different relative weightings of $m_c = 0$ or ± 1. The results of Fig. 4 imply that, since Auger electrons with different values of m_A have different angular distributions,[14,15] we expect that each pairwise coincidence angular distribution will have a different profile. In particular, the asymmetry with respect to the surface normal observed in the case of analyzers 1, 2, 4, and 5 suggests that the $+m$ and $-m$ components are not equally represented in the coincidence Auger electron angular distributions. Experiments performed on isolated atoms have already shown that by measuring coincidence angular distributions (AR-APECS), different ''alignment'' for the intermediate core hole state can be selected.[17] The validity of these ideas for the solid state must be verified by detailed calculations of the AR-APECS angular distributions that, to be more realistic, might have to include some degree of coherence between the two scattered wave functions. Such calculations are not yet available.

In summary, our results show that AR-APECS from solid surfaces provides a way to perform AED with enhanced surface sensitivity and a means to probe the core hole/Auger decay mechanism in the solid matter by taking advantage of the momentum selectivity of the two electrons. Conventional AED and XPD can be used to elucidate the mechanism underlying the core hole generation process[14] and add insight into the multiplet structure and Auger line shape.[18] AR-APECS provides a way to disentangle source function generated effects from diffraction phenomena, i.e., one can explore specific magnetic sublevels in the wave function representing the emitted Auger electron. Finally, we note that AR-APECS, by detecting the coincident photoelectron, preserves the chirality of the ionization event and then opens the possibility to measure dichroic effects in the Auger emission, thus providing insight into the study of magnetic systems.

The authors are grateful to the ALOISA beamline staff members for the valuable support provided during the AR-APECS experiments performed at the ELETTRA synchrotron radiation facility, and they are also indebted to INFM for financial support provided through the ''Supporto ELETTRA'' program. Two of us (M.B. and R.A.B.) acknowledge supported by the NSE under Grant No. DMR98-01681.

[1] H. W. Haak, G. A. Sawatzky, and T. D. Thomas, Phys. Rev. Lett. **41**, 1825 (1978).
[2] R. A. Bartynski, S. Yang, S. L. Hulbert, C. C. Kao, M. Weinert, and D. M. Zehner, Phys. Rev. Lett. **68**, 2247 (1992).
[3] D. A. Arena, R. A. Bartynski, S. L. Hulbert, R. Nayak, and A. H. Weiss, Phys. Rev. B **63**, 155102 (2001).
[4] E. Jensen, R. A. Bartynski, S. L. Hulbert, E. D. Johnson, and C. C. Kao, Phys. Rev. B **45**, 13 636 (1992).
[5] E. Jensen, R. A. Bartynski, S. L. Hulbert, E. D. Johnson, and R. F. Garrett, Phys. Rev. Lett. **62**, 71 (1989).
[6] S. Rioual, B. Rouvellou, I. Avaldi, G. Battera, R. Camiloni, G. Stefani, and G. Turri, Phys. Rev. Lett. **86**, 1470 (2001).
[7] R. Gotter, A. Attili, L. Marassi, R. A. B. D. Arena, D. Cvetko, L. Floreano, S. Iacobucci, A. Morgante, P. Luches, A. Ruocco, F. Tommasini, and G. Stefani, Appl. of Acc. Res. Ind. **PC475**, 106 (1999).
[8] R. Gotter, A. Ruocco, A. Morgante, D. Cvetko, L. Floreano, F. Tommasini, and G. Stefani, Nucl. Instrum. Methods Phys. Res. A **467–468**, 1468 (2001).
[9] R. M. Tromp, R. J. Hammers, and J. E. Demuth, Phys. Rev. Lett. **55**, 1303 (1985).
[10] M. A. van Hove and Y. Chen, computer code MSCD, version 1.37 (LBNL, Berkely, CA, 1998).
[11] X. Torrelles, H. A. ver der Vegt, V. H. Etgens, P. Fajardo, J. Alvarez, and S. Ferrer, Surf. Sci. **364**, 242 (1996).
[12] G. A. Sawatzky, in *Auger Electron Spectroscopy*, edited by C. L. Bryant and R. P. Messmer (Academic, Boston, 1988), p. 167.
[13] E. Antonides, E. C. Janse, and G. A. Sawatzky, Phys. Rev. B **15**, 1669 (1977).
[14] D. E. Ramaker, R. A. Fry, and Y. U. Idzerda, J. Electron Spectrosc. Relat. Phenom. **72**, 169 (1995).
[15] Y. U. Idzerda, Surf. Rev. Lett. **4**, 161 (1997).
[16] P. J. Feibelman and E. J. McGuire, Phys. Rev. B **17**, 690 (1978).
[17] V. Schmidt, Nucl. Instrum. Methods Phys. Res. B **87**, 241 (1994).
[18] D. E. Ramaker, H. Yang, and Y. U. Idzerda, J. Electron Spectrosc. Relat. Phenom. **68**, 63 (1994).